# Closed Loop Resuspension Flume

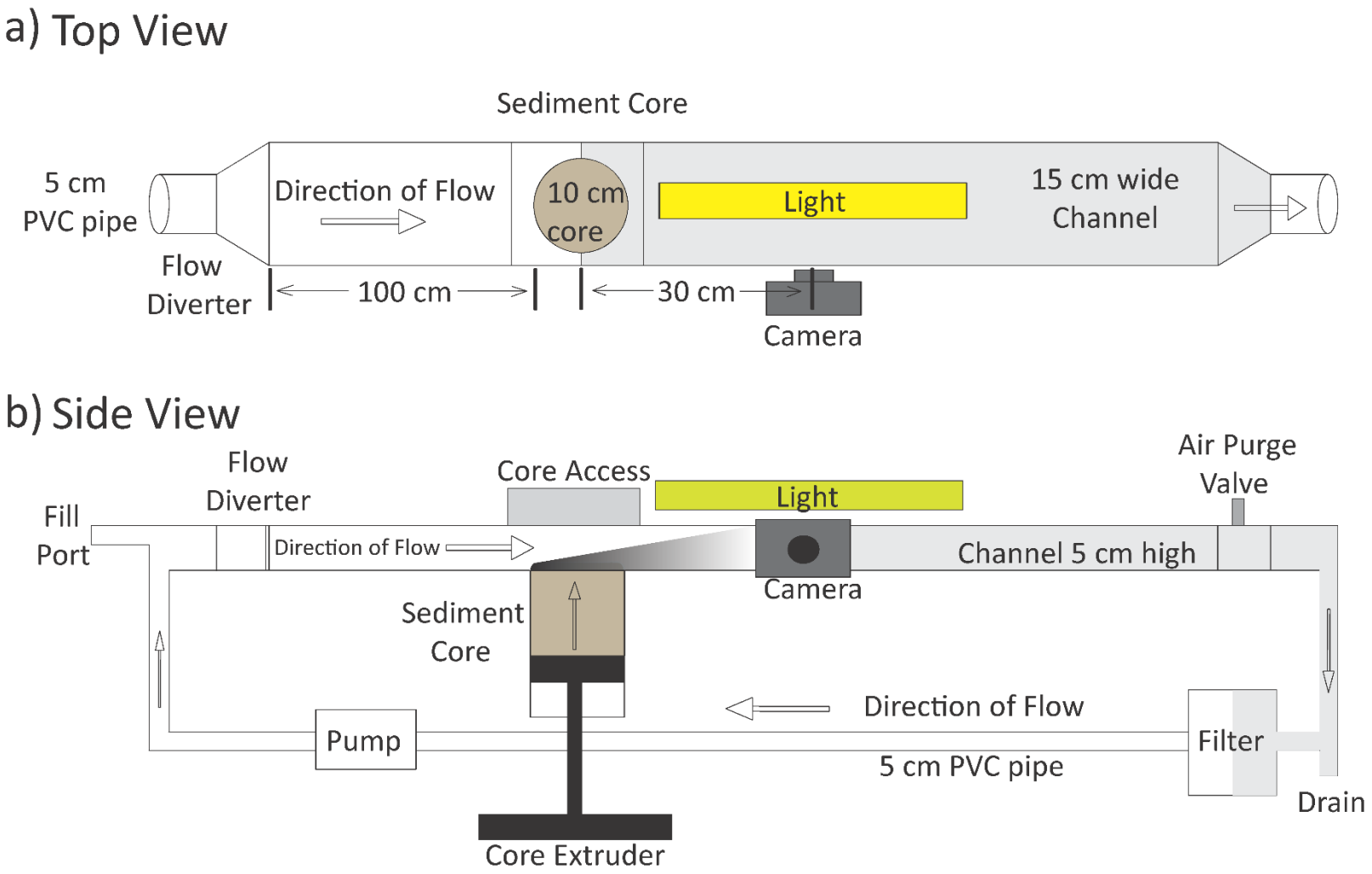


Supplemental Figure 1: Schematic diagram of the closed loop resuspension flume.

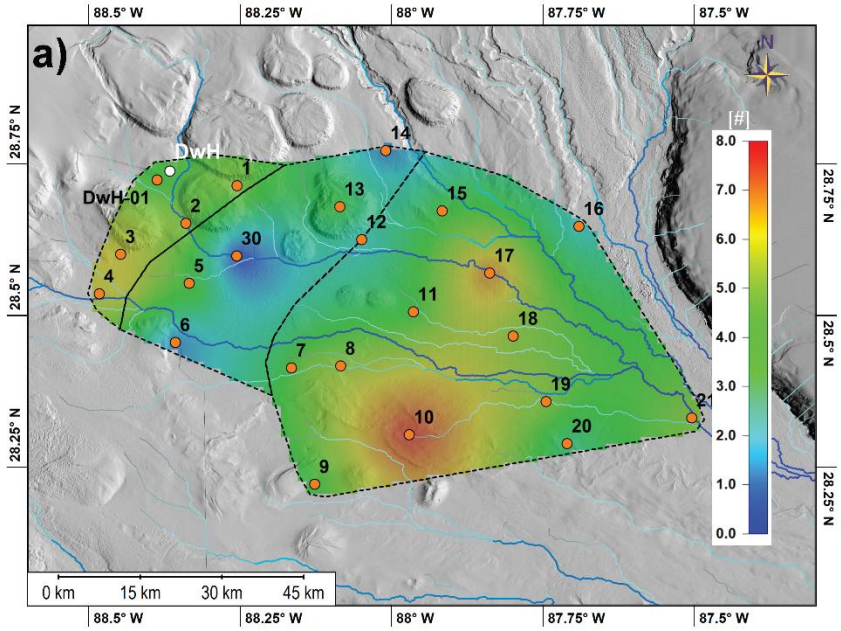


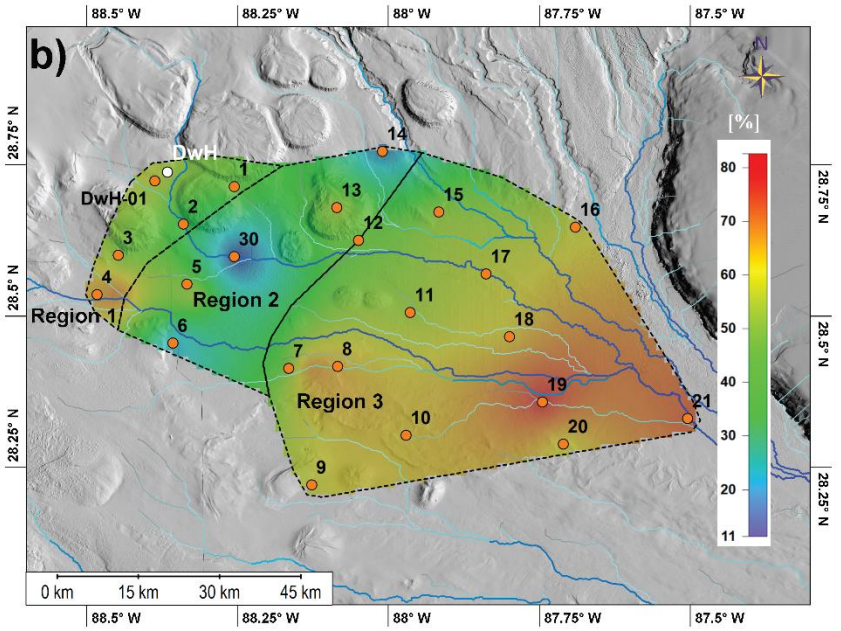


Supplemental Figure 2:

Top left (a): number of pulse events between 1950 and 2018, top right (b): percent of sediment accumulation that occurred during pulsed events between 1950 and 2018, bottom right (c): $^{210}Pb_{xs}$ average mass accumulation rates between 1950 and 2018.

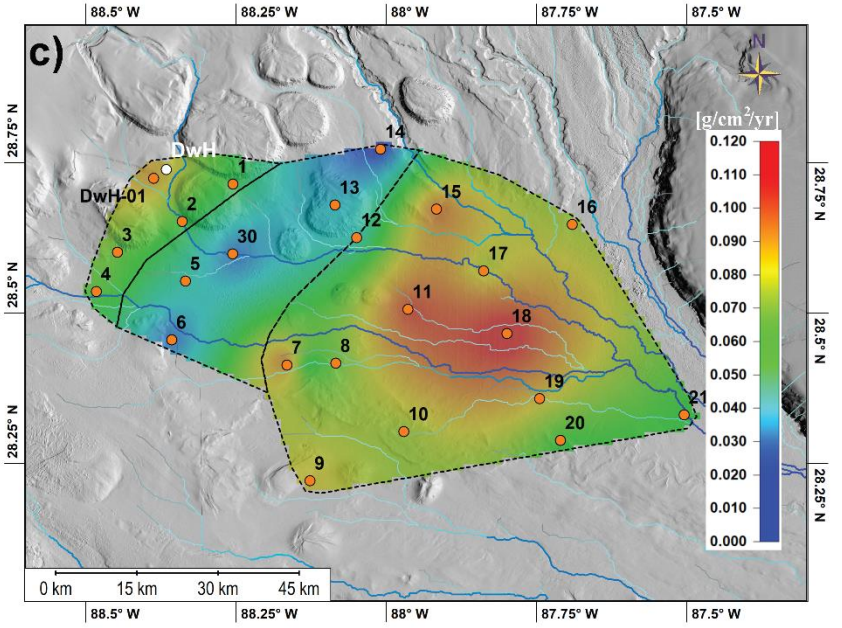

# Region 1

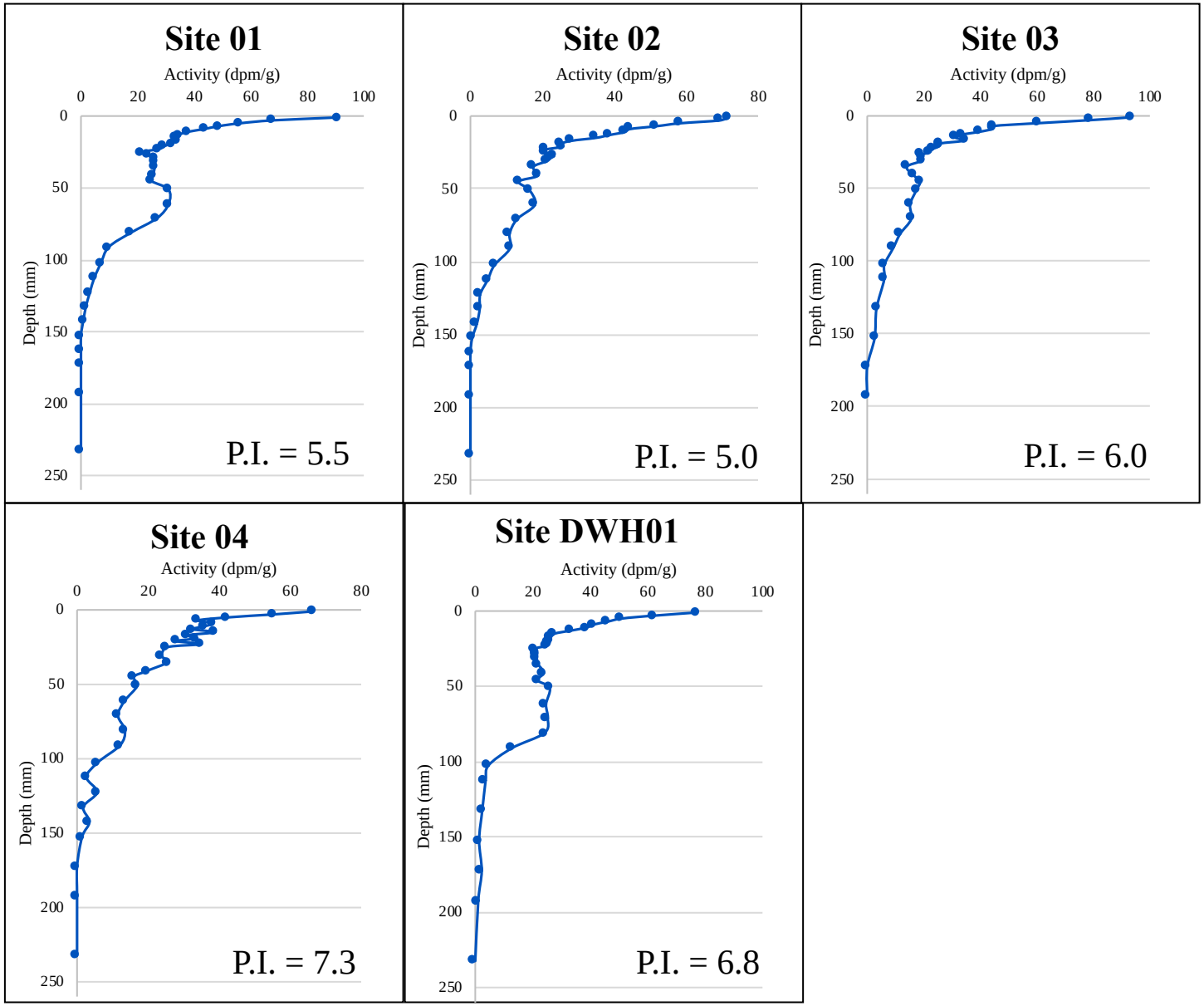


Supplemental Figure 3a: Profiles of $^{210}Pb_{xs}$ activities with depth for Region 1. P.I. indicates pulse index.

# Region 2

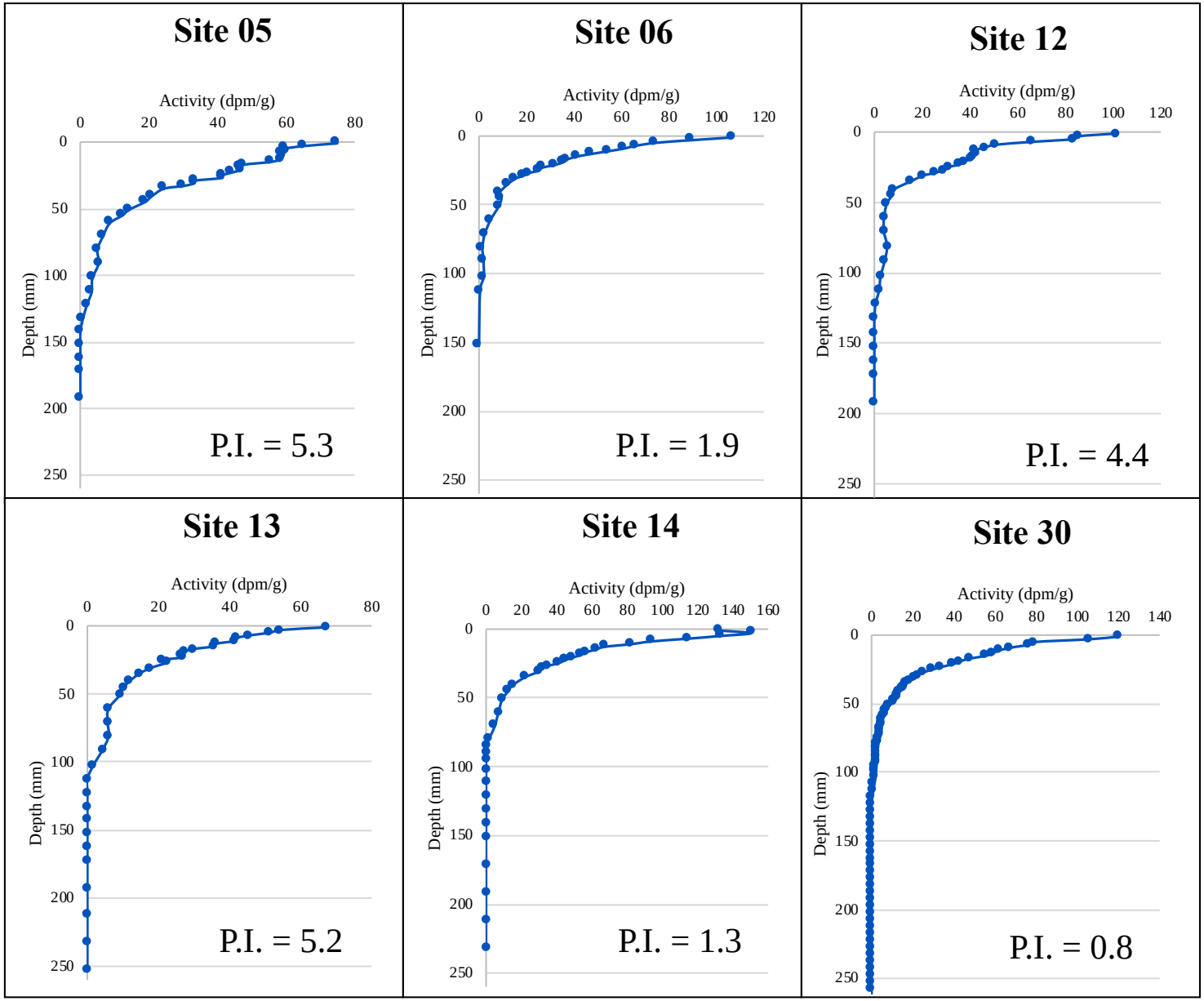


Supplemental Figure 3b: Profiles of $^{210}Pb_{xs}$ activities with depth for Region 2. P.I. indicates pulse index.

Supplemental Figure 3c:

Profiles of $^{210}Pb_{xs}$ activities with depth for Region 3. P.I. indicates pulse index.

# Region 3

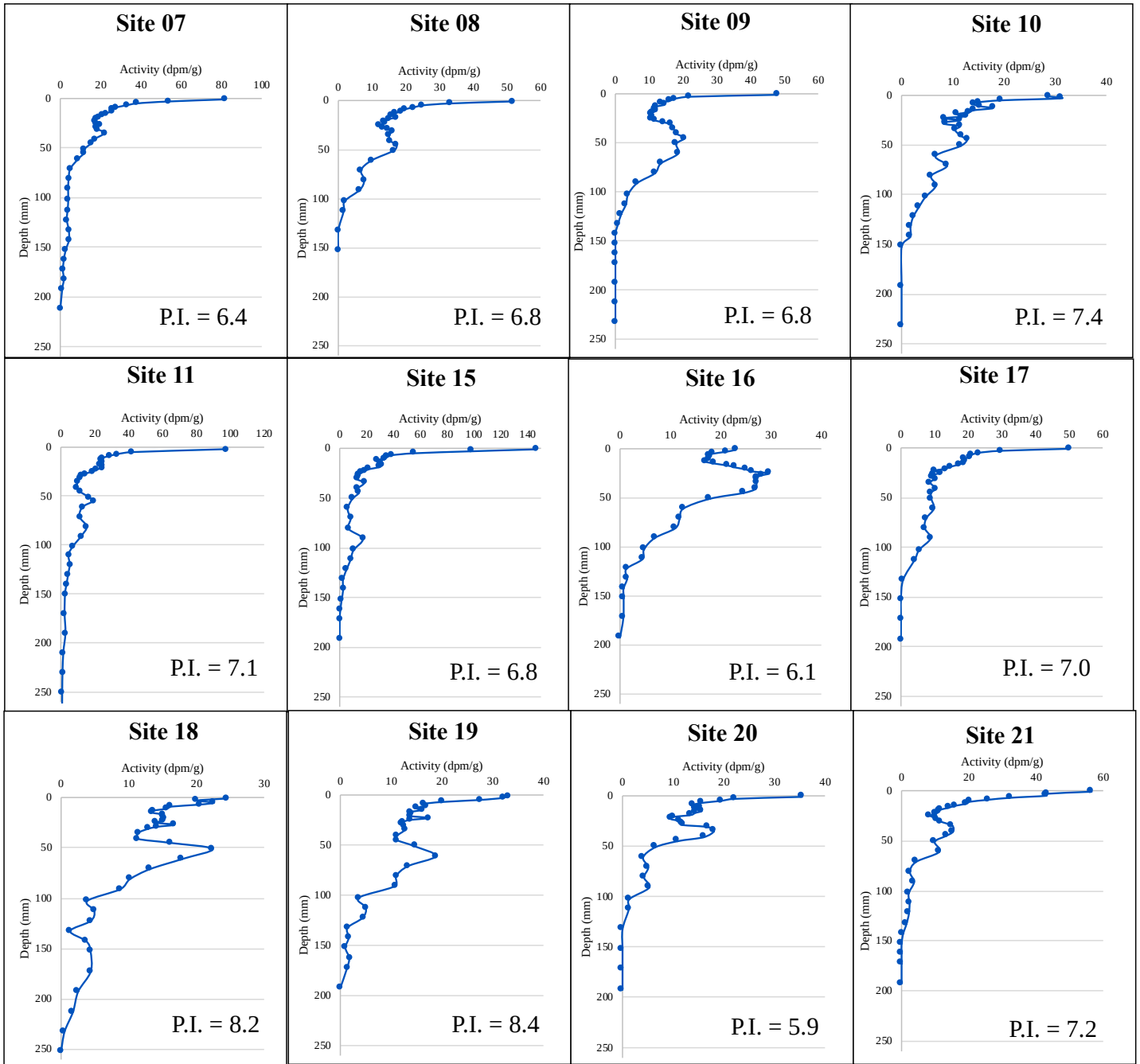

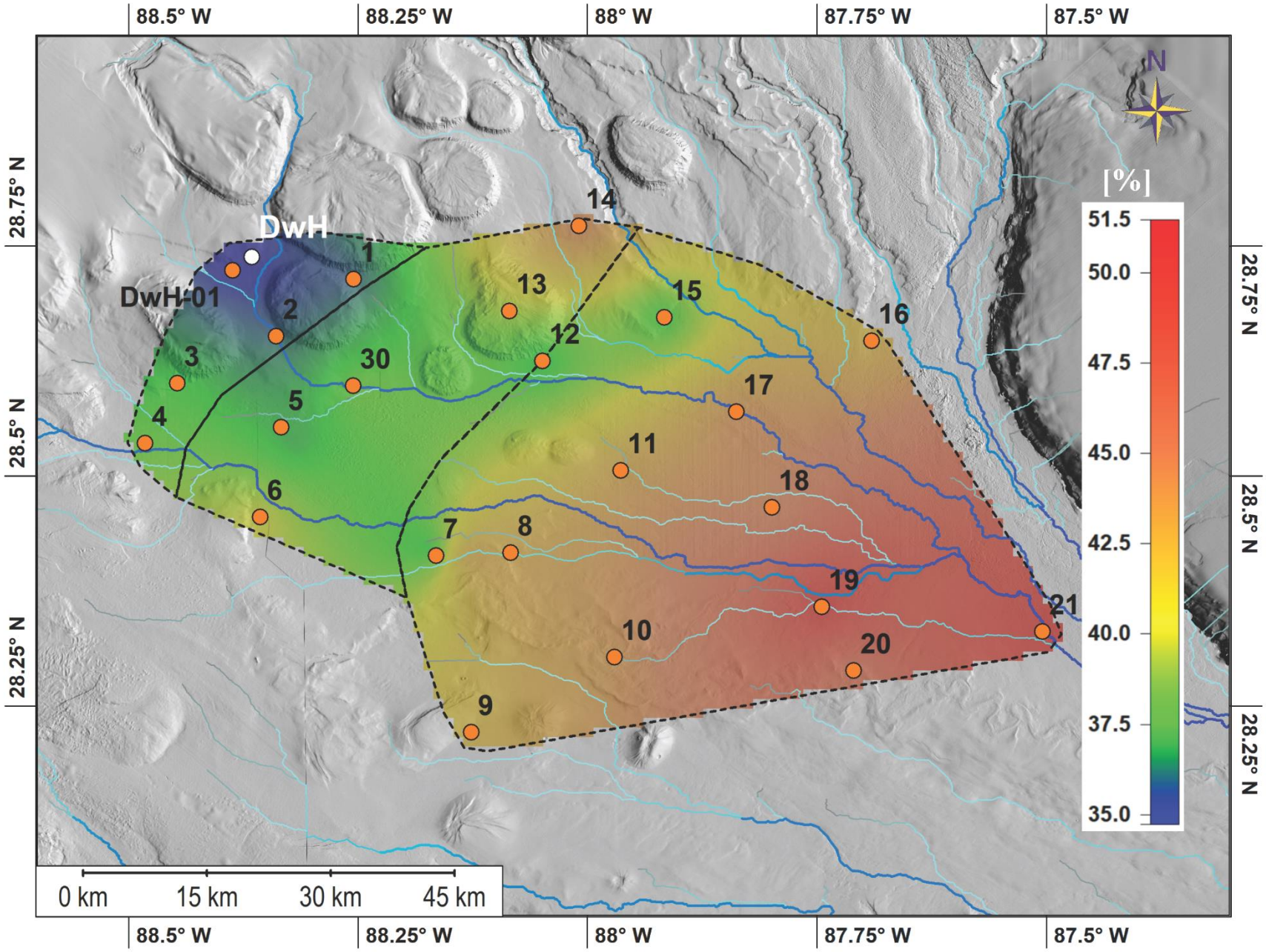


Supplemental Figure 4: Percent carbonate in surface Sediments.

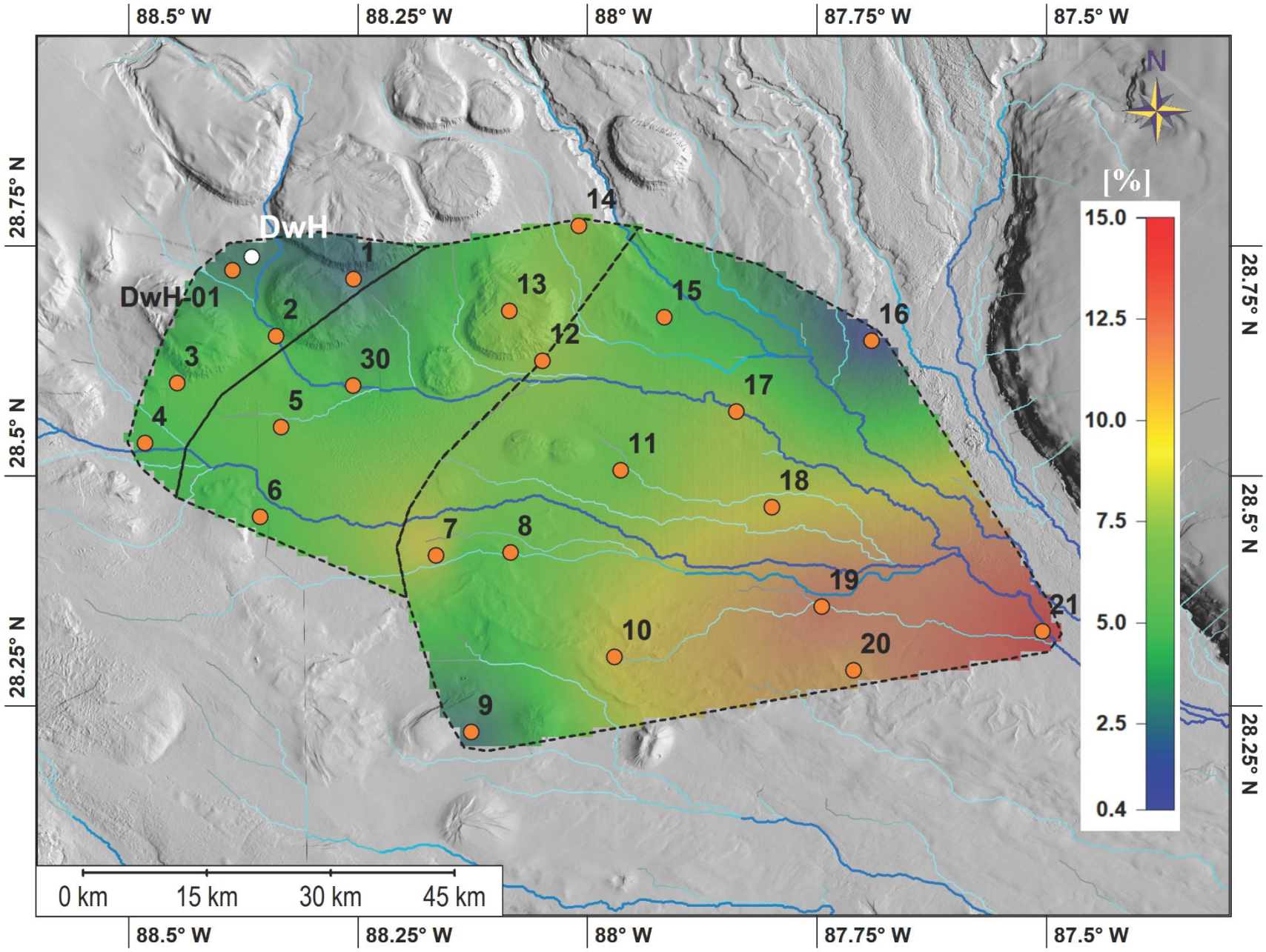


Supplemental Figure 5: Percent sand concentration in surface sediments.

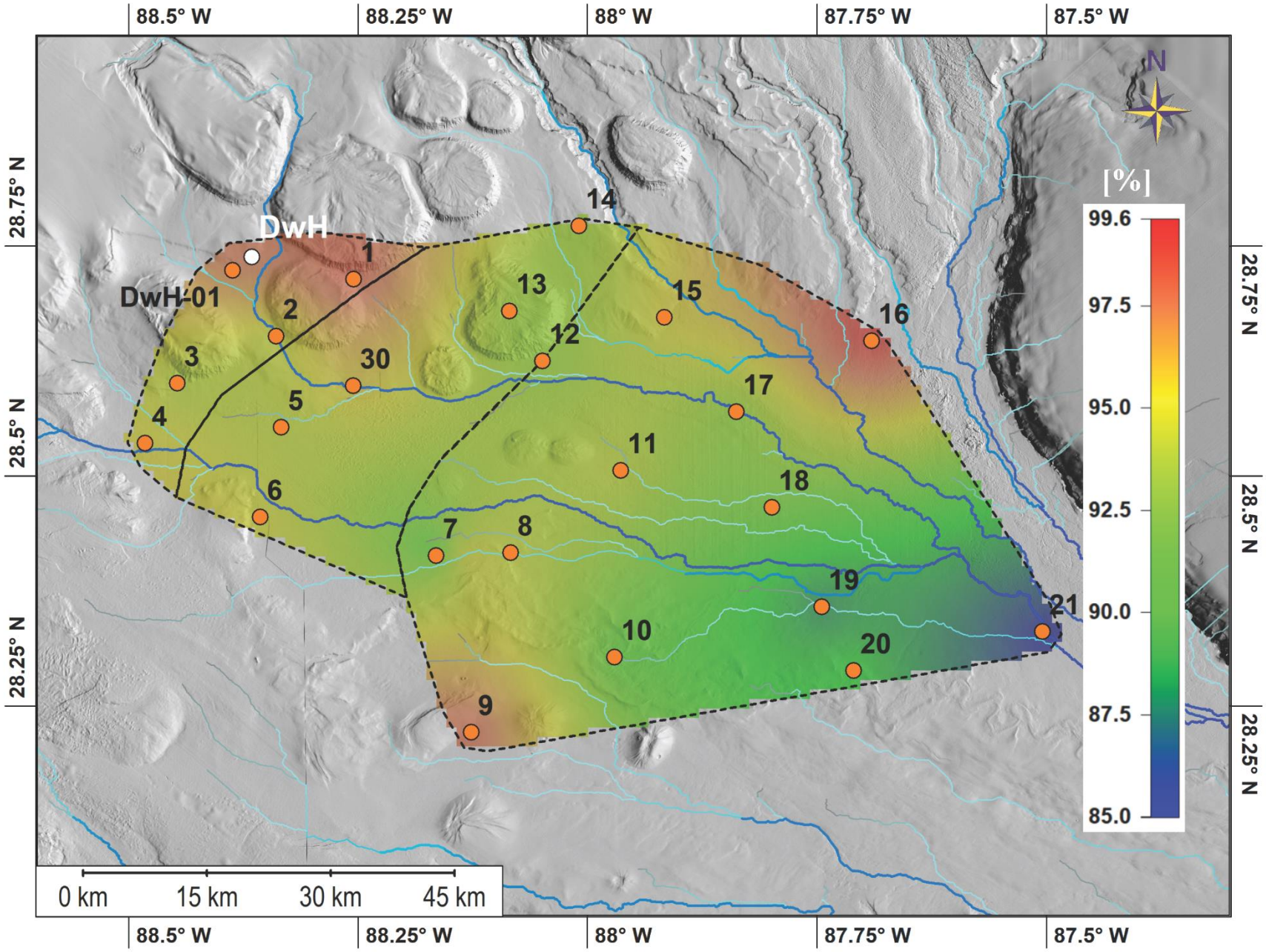


Supplemental Figure 6: Percent mud in surface sediments.

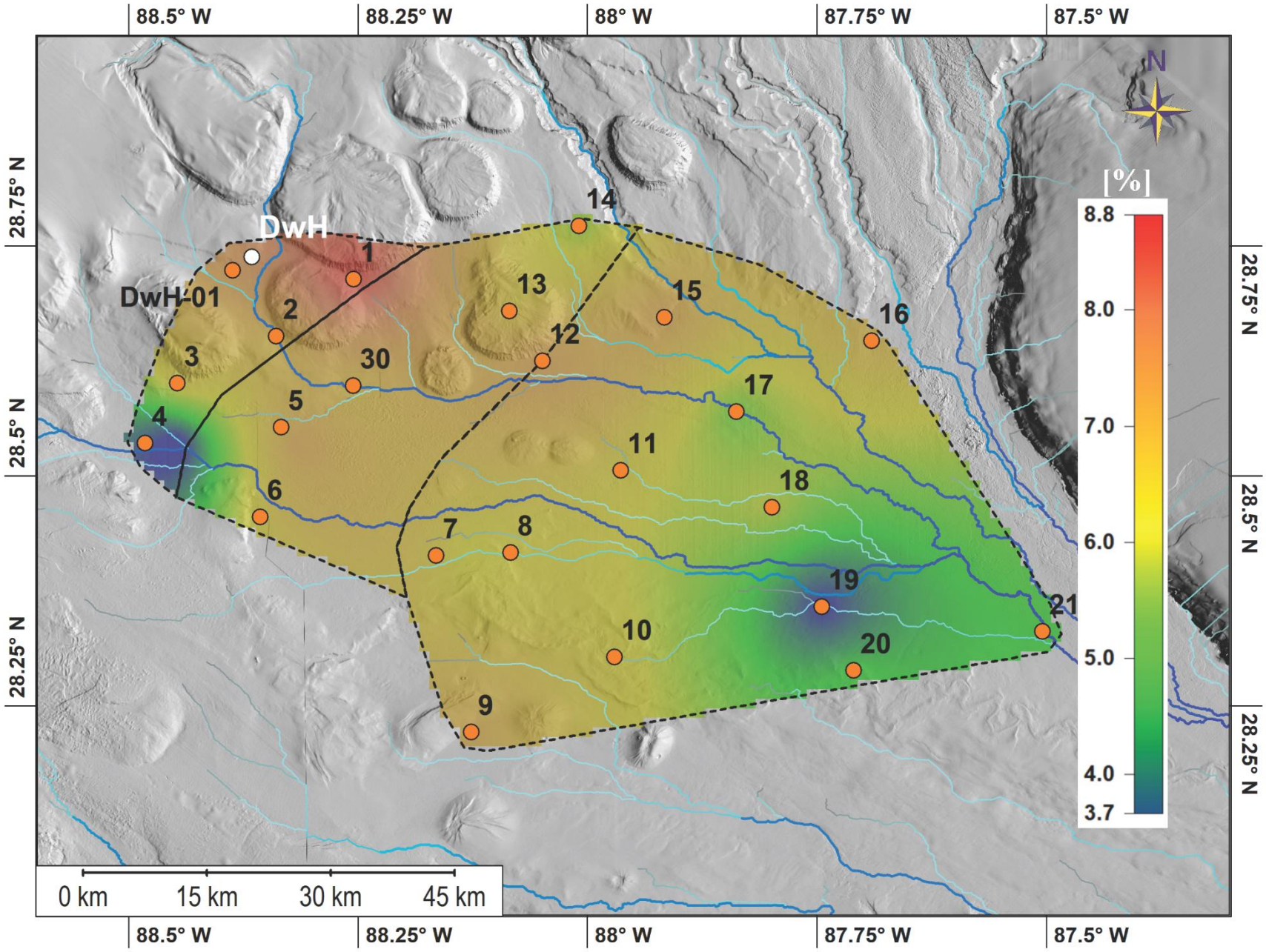


Supplemental Figure 7: Percent total organic matter in surface sediments.

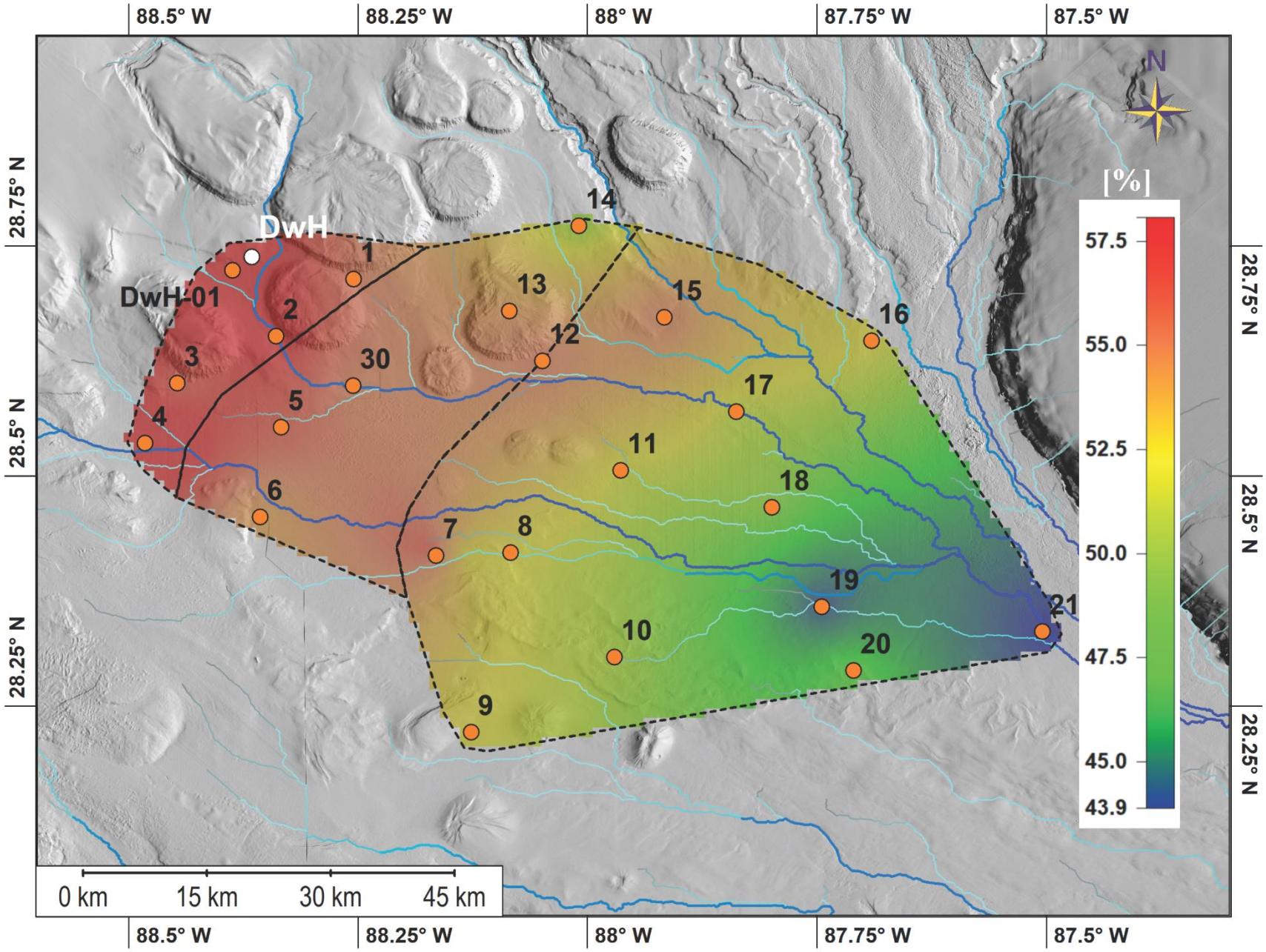


Supplemental Figure 8: Percent terrigenous material in surface sediments.

Supplemental Figure 9a:

Relative abundance (%) of hydrocarbon compound groups by sediment intervals in the northern GoM (sites DWH, 30, and 1-10). Shac areas on the x-axis correspond to the time per 2010-2013.

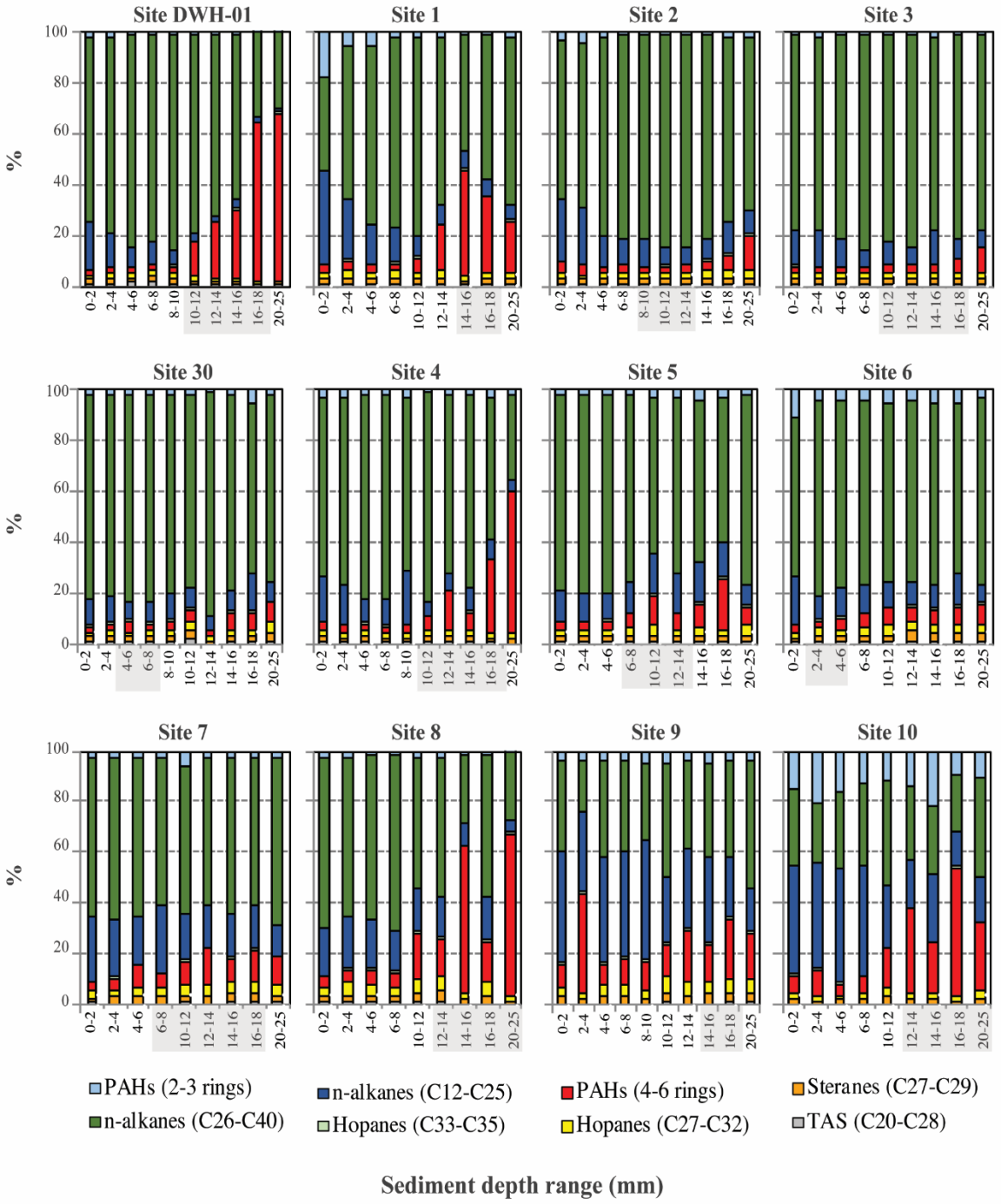

Supplemental Figure 9b:

Relative abundance (%) of hydrocarbon compound groups by sediment intervals in the northern GoM (sites 11-21, and 24). Shaded areas on the x-axis correspond to the time period 2010-2013.

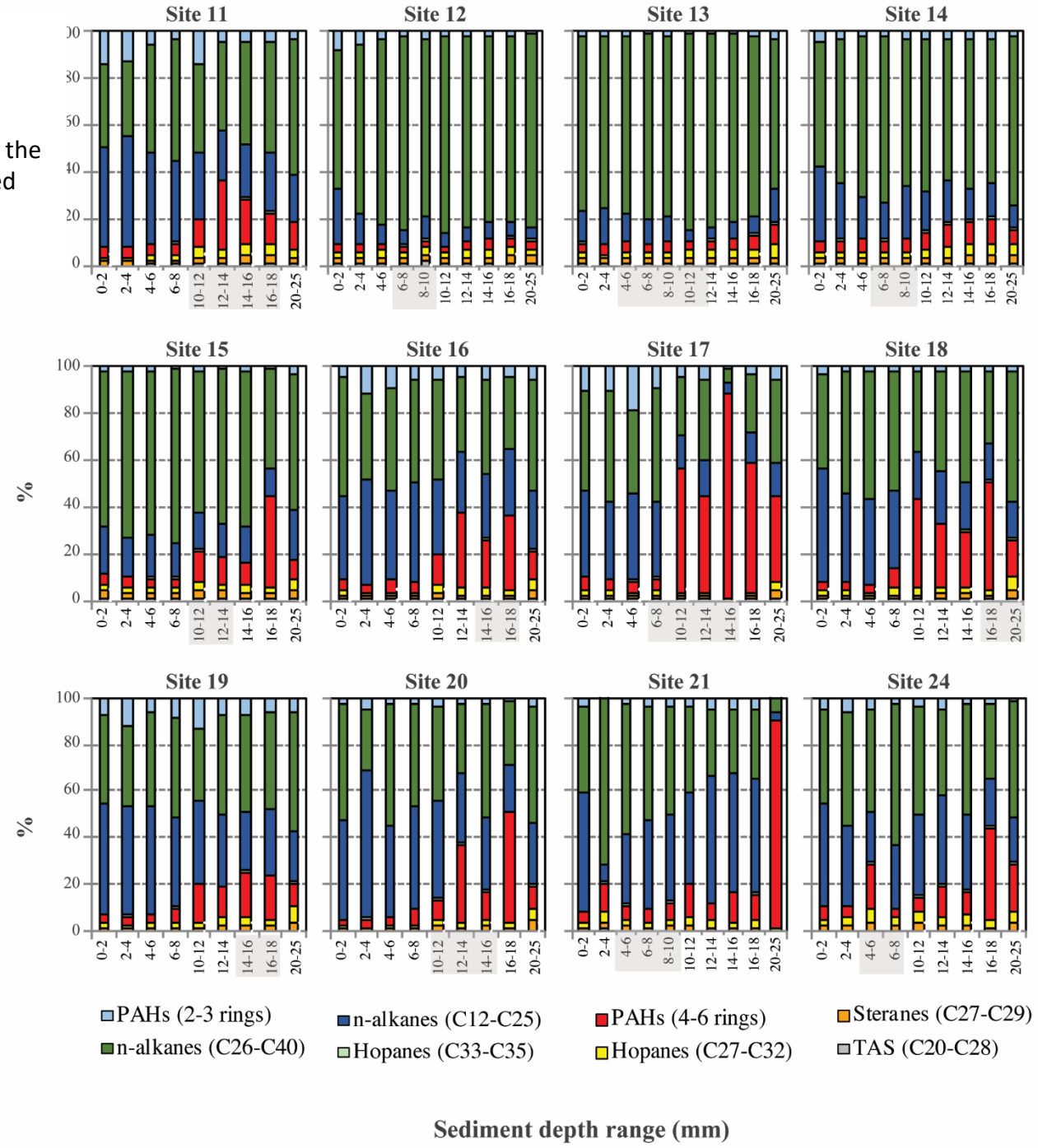

Supplemental Figure 10a:

LMW PAH (2-3 rings) concentration profiles in the study sites located in the northern GoM. Red circles denote samples with DwH oil-residues as the potential major source, green circles indicate samples with mixed hydrocarbons sources including DwH oil-residues, and black circles indicate other unknown sources.

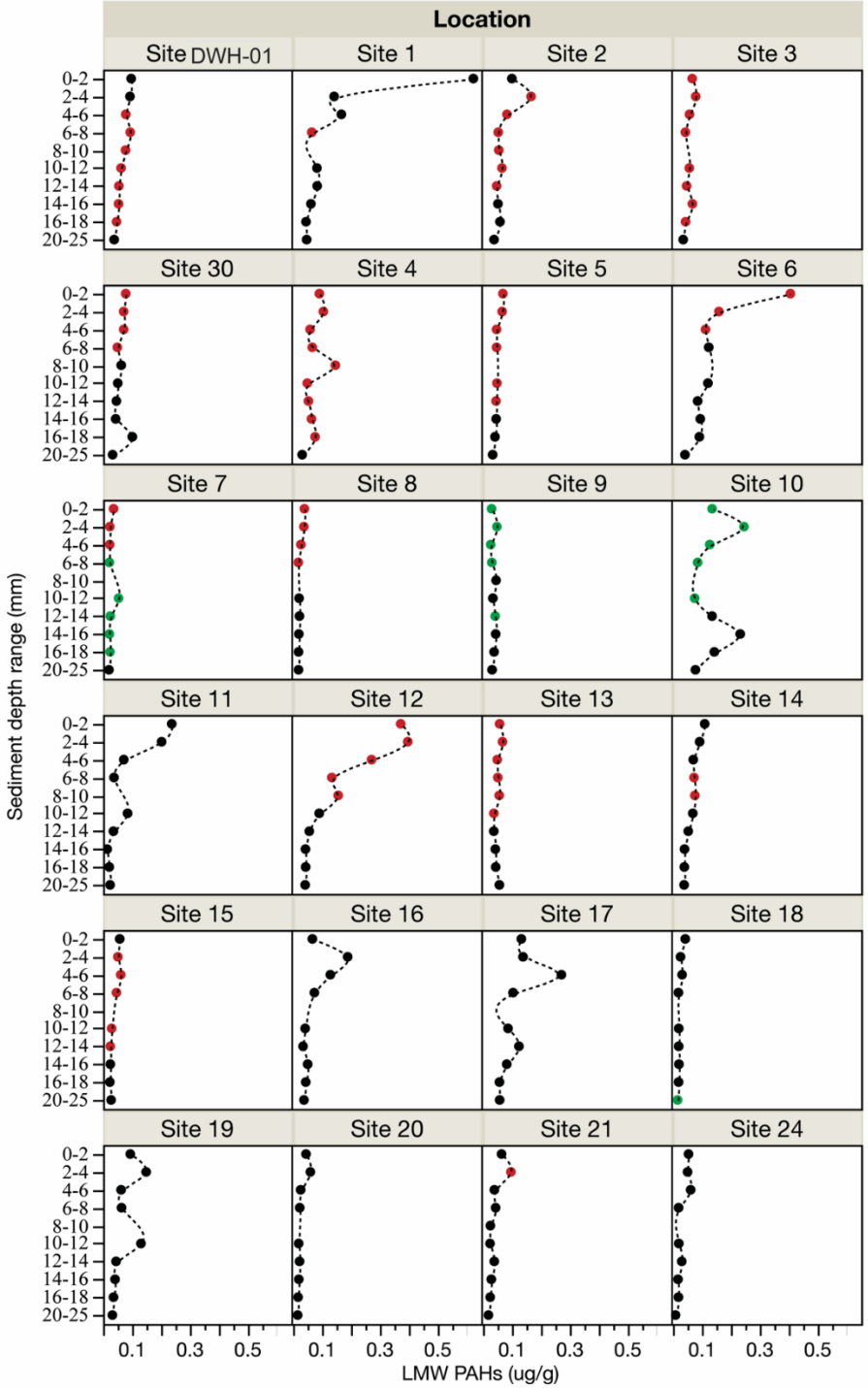

Supplemental Figure 10b:

HMW PAH (4-6 rings) concentration profiles in the study sites located in the northern GoM. Red circles denote samples with DwH oil-residues as the potential major source, green circles indicate samples with mixed hydrocarbons sources including DwH oil-residues, and black circles indicate other unknown sources.

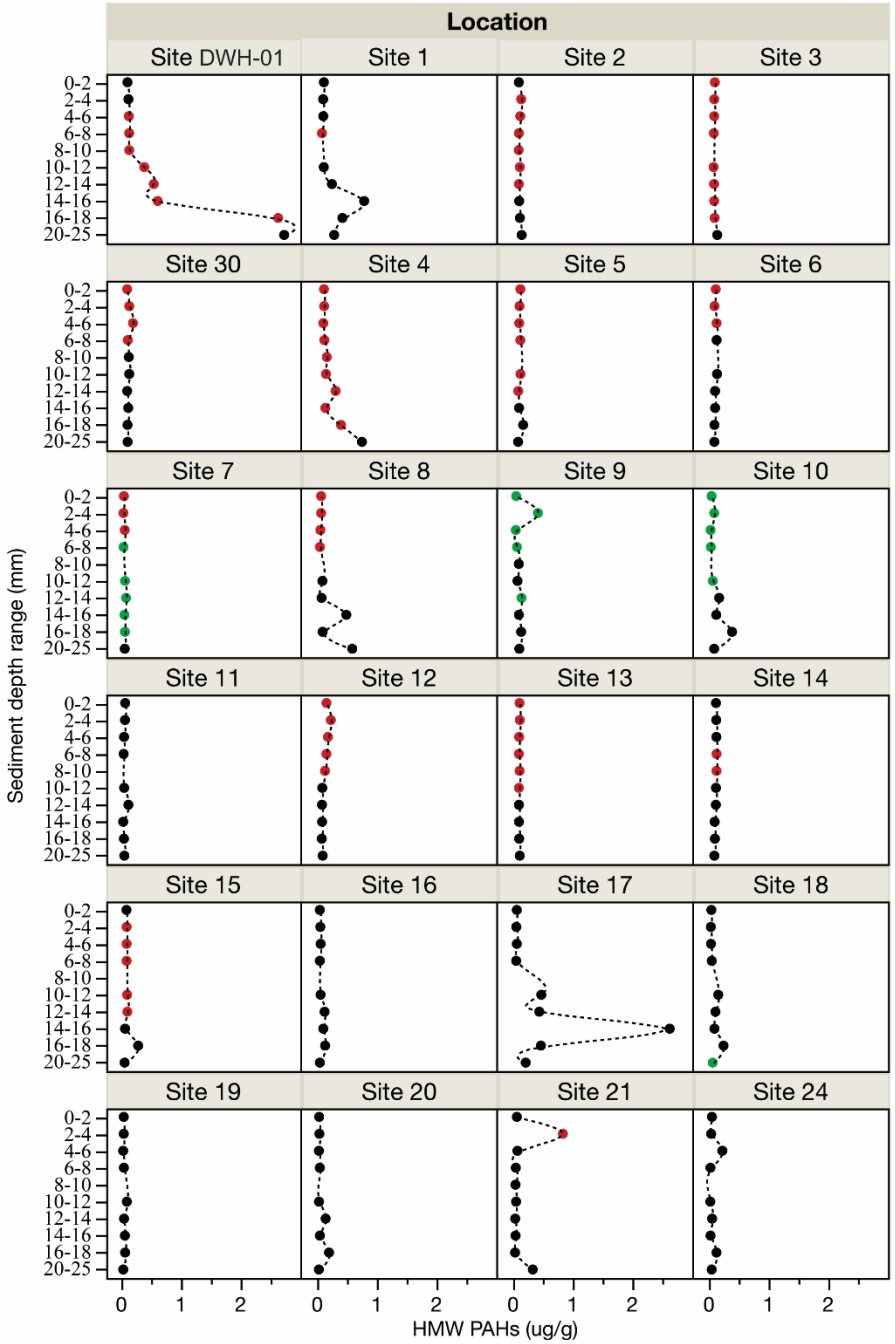

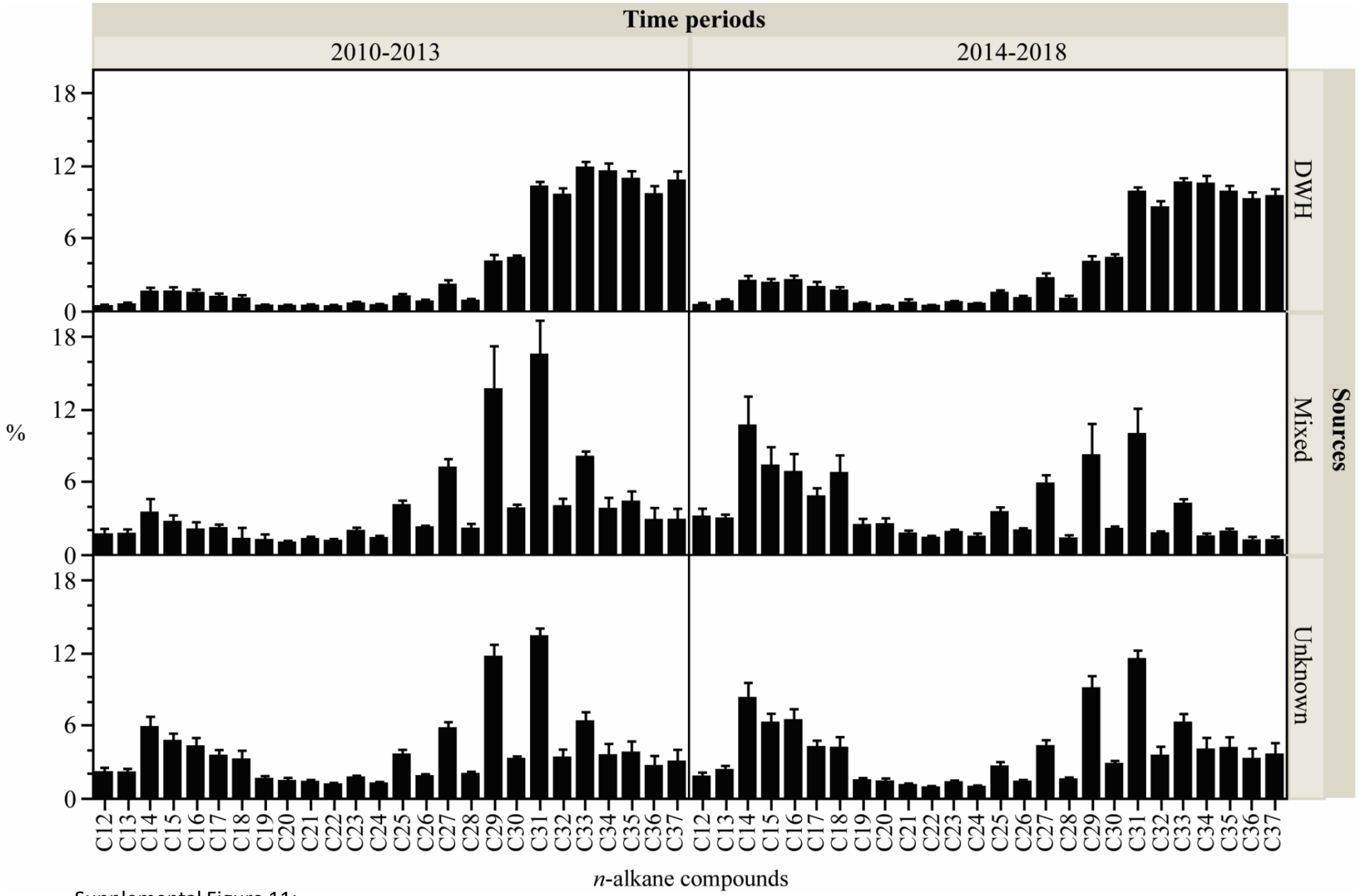


Supplemental Figure 11:
Distribution patterns of *n*-alkanes for three potential sources identified in the PCA analysis (Figure 11) and Cross plots (Figure 12) of diagnostic ratios. Data shown as mean ± 95% confidence interval.

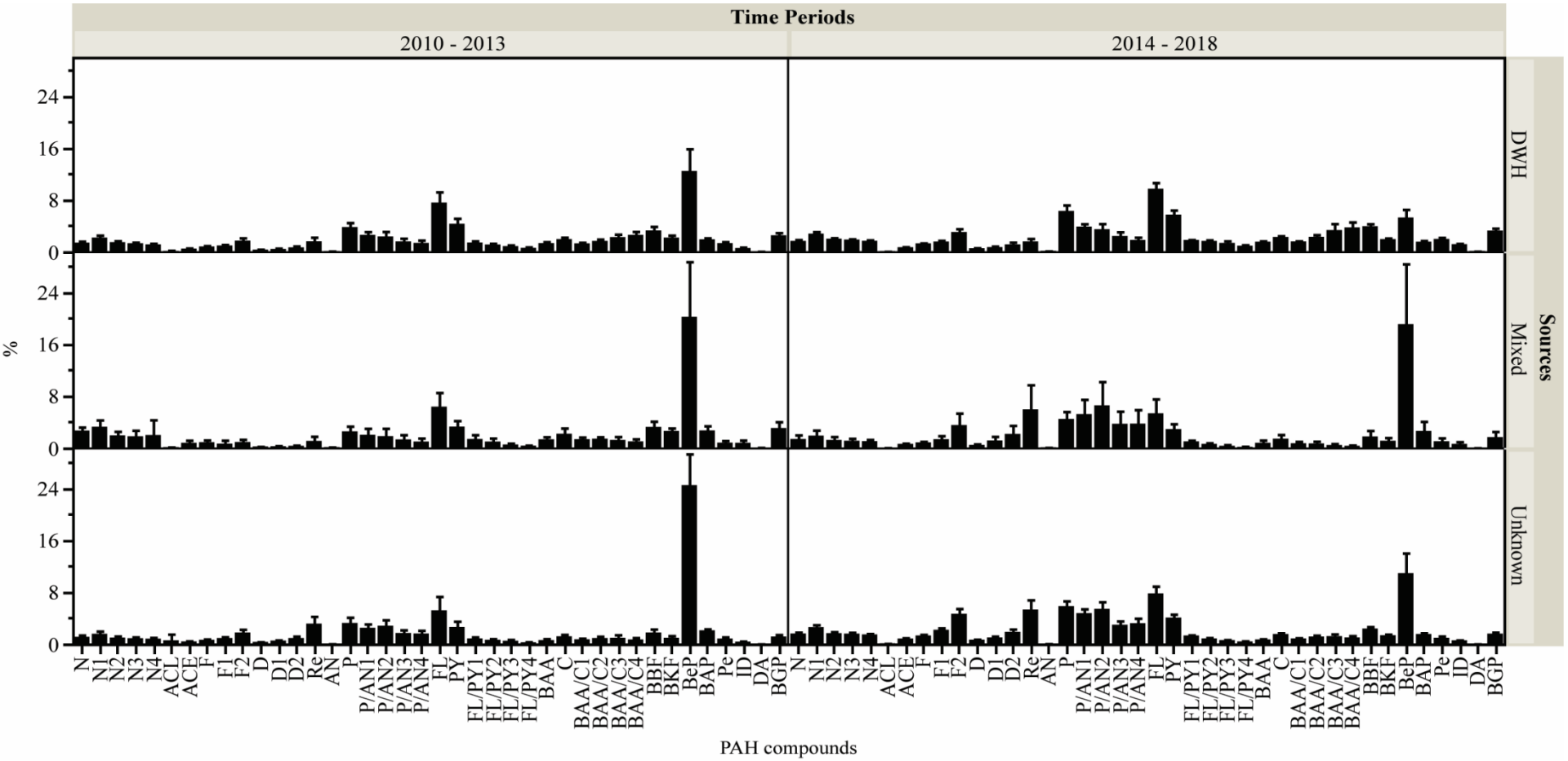


Supplemental Figure 12:

Distribution patterns of PAHs for three potential sources identified in the PCA analysis (Figure 11) and Cross plots (Figure 12) of diagnostic ratios. Data shown as mean ± 95% confidence interval.

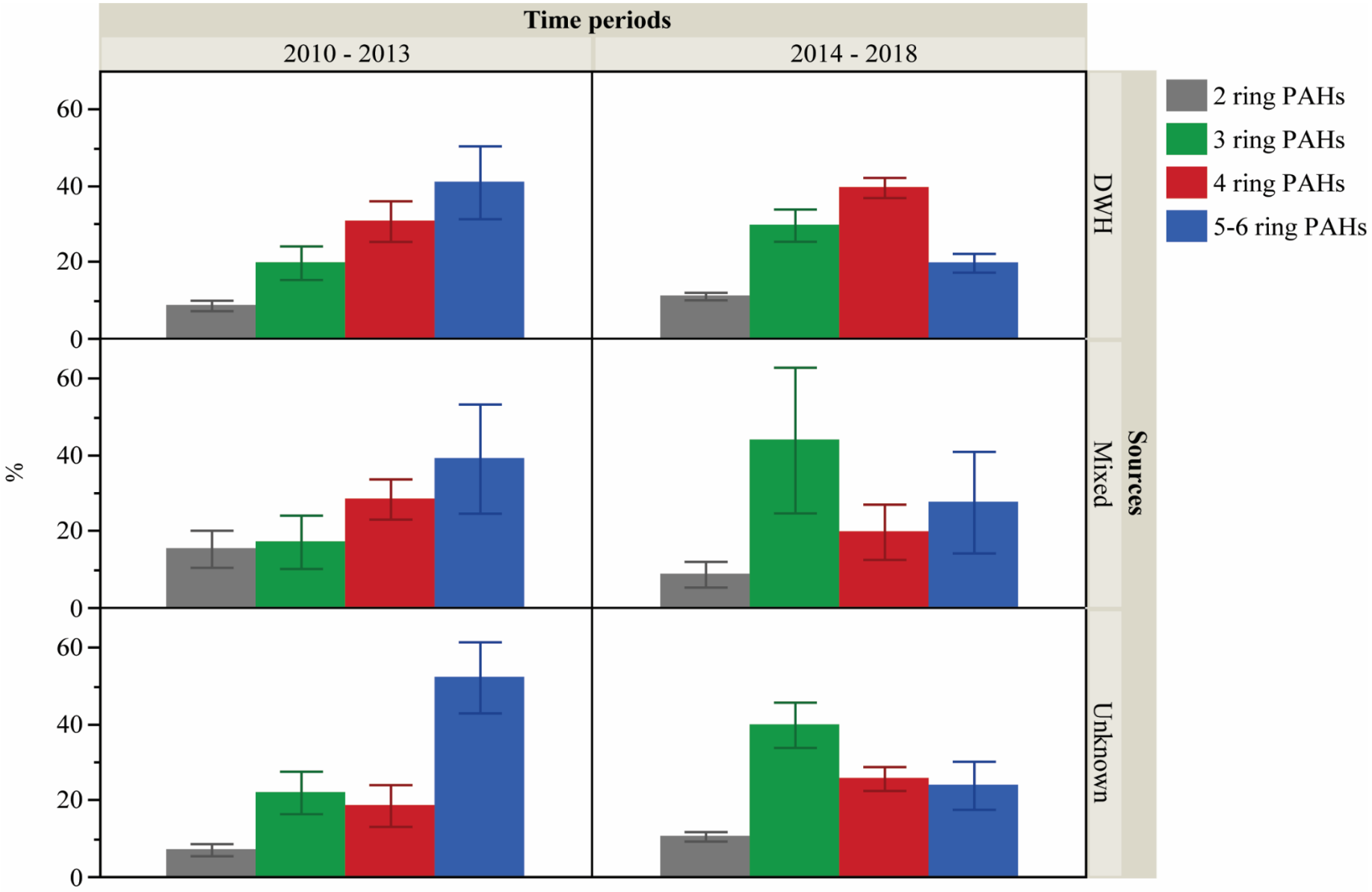


Supplemental Figure 13: Abundance (%) of PAHs by ring number for three potential sources identified in the PCA analysis (Figure 11) and Cross plots (Figure 12) of diagnostic ratios. Data shown as mean ± 95% confidence interval.

Supplemental Table 1:

$^{210}Pb_{xs}$ average mass accumulation data and Pulse Index values results

| Site | Average MAR: 1950-2018 | # Pulse events: 1950-2018 | % of Accumulation that is pulsed: 1950-2018 | Pulse Index | Average MAR: 2006-2009 | Average MAR: 2010-2013 | Average MAR: 2014-2018 | Region |
|---|---|---|---|---|---|---|---|---|
| | $g/cm^2/yr$ | # | % | | $g/cm^2/yr$ | $g/cm^2/yr$ | $g/cm^2/yr$ | |
| 1 | 0.057 | 5 | 47 | 5.5 | 0.093 | 0.081 | 0.054 | 1 |
| 2 | 0.060 | 5 | 38 | 5.0 | 0.064 | 0.049 | 0.039 | 1 |
| 3 | 0.065 | 6 | 48 | 6.0 | 0.082 | 0.063 | 0.04 | 1 |
| 4 | 0.062 | 6 | 72 | 7.3 | 0.067 | 0.062 | 0.056 | 1 |
| 5 | 0.042 | 4 | 54 | 5.3 | 0.034 | 0.034 | 0.035 | 2 |
| 6 | 0.027 | 1 | 14 | 1.9 | 0.02 | 0.019 | 0.017 | 2 |
| 7 | 0.096 | 4 | 46 | 6.4 | 0.087 | 0.073 | 0.048 | 3 |
| 8 | 0.057 | 5 | 68 | 6.8 | 0.089 | 0.08 | 0.056 | 3 |
| 9 | 0.082 | 4 | 59 | 6.8 | 0.098 | 0.157 | 0.117 | 3 |
| 10 | 0.073 | 8 | 62 | 7.4 | 0.112 | 0.091 | 0.075 | 3 |
| 11 | 0.107 | 4 | 53 | 7.1 | 0.102 | 0.092 | 0.053 | 3 |
| 12 | 0.042 | 2 | 46 | 4.4 | 0.03 | 0.023 | 0.021 | 2 |
| 13 | 0.039 | 4 | 54 | 5.2 | 0.032 | 0.031 | 0.028 | 2 |
| 14 | 0.020 | 1 | 8 | 1.3 | 0.018 | 0.016 | 0.014 | 2 |
| 15 | 0.098 | 4 | 51 | 6.8 | 0.066 | 0.069 | 0.03 | 3 |
| 16 | 0.074 | 2 | 58 | 6.1 | 0.07 | 0.096 | 0.138 | 3 |
| 17 | 0.074 | 7 | 57 | 7.0 | 0.092 | 0.072 | 0.057 | 3 |
| 18 | 0.119 | 5 | 61 | 8.2 | 0.15 | 0.142 | 0.137 | 3 |
| 19 | 0.083 | 5 | 82 | 8.4 | 0.124 | 0.118 | 0.093 | 3 |
| 20 | 0.060 | 3 | 59 | 5.9 | 0.086 | 0.077 | 0.06 | 3 |
| 21 | 0.059 | 5 | 75 | 7.2 | 0.063 | 0.045 | 0.032 | 3 |
| 30 | 0.028 | 0 | 0 | 0.8 | 0.021 | 0.026 | 0.019 | 2 |
| DwH-01 | 0.089 | 4 | 57 | 6.8 | 0.108 | 0.078 | 0.052 | 1 |

Supplemental Table 2a: Hydrocarbon compounds (hopanes, steranes, TAS) analyzed with analytical parameters.

| Compounds | Abbreviation | Precursor ion (m/z) | Quantitation ion (m/z) | CE 1 (eV) | Confirmation ion (m/z) | CE 2 (eV) | RT (min) | RT window width (± RT min) |
|---|---|---|---|---|---|---|---|---|
| **Hopanes** | | | | | | | | |
| 18α(H)-22,29,30-trisnorneohopane | T11 | 370.5 | 191.2 | 10 | 121.0 | 10 | 38.7 | 37.7-39.7 |
| 17α(H)-22,29,30-trisnorhopane | T12 | 370.5 | 191.2 | 10 | 121.0 | 10 | 39.4 | 38.4-40.4 |
| 17αβ,21βα 28,30-Bisnorhopane | T14a | 384.5 | 191.2 | 10 | 121.0 | 10 | 40.8 | 39.8-41.8 |
| 30-norhopane; 18α(H)-30-Norneohopane | T15,T16 | 398.5 | 191.2 | 10 | 121.0 | 10 | 41.5 | 40.5-42.5 |
| 30-Normoretane | T17 | 398.5 | 191.2 | 10 | 121.0 | 10 | 42.4 | 41.4-43.4 |
| 17α(H),21β(H)-hopane | T19 | 412.5 | 191.2 | 10 | 121.0 | 10 | 42.9 | 41.9-43.9 |
| 17β(H),21α(H)-moretane | T20 | 412.5 | 191.2 | 10 | 121.0 | 10 | 43.5 | 42.5-44.5 |
| 17α(H),21β(H)-22S-homohopane | T21 | 426.5 | 191.2 | 10 | 121.0 | 10 | 44.4 | 43.4-45.4 |
| 17α(H),21β(H)-22R-homohopane | T22 | 426.5 | 191.2 | 10 | 121.0 | 10 | 44.6 | 43.6-45.6 |
| 17α(H),21β(H)-22S-bishomohopane | T26 | 440.5 | 191.2 | 10 | 121.0 | 10 | 45.6 | 4.5-46.5 |
| 17α(H),21β(H)-22R-bishomohopane | T27 | 440.5 | 191.2 | 10 | 121.0 | 10 | 45.8 | 44.7-46.7 |
| 17α(H),21β(H)-22S-trishomohopane | T30 | 454.5 | 191.2 | 10 | 121.0 | 10 | 46.7 | 45.7-47.7 |
| 17α(H),21β(H)-22R-trishomohopane | T31 | 454.5 | 191.2 | 10 | 121.0 | 10 | 47.0 | 45.9-47.9 |
| 17α(H),21β(H)-22S-tetrakishomohopane | T32 | 468.5 | 191.2 | 10 | 121.0 | 10 | 47.8 | 46.8-48.8 |
| 17α(H),21β(H)-22R-tetrakishomohopane | T33 | 468.5 | 191.2 | 10 | 121.0 | 10 | 48.2 | 47.1-49.1 |
| 17α(H),21β(H)-22S-pentakishomohopane | T34 | 482.5 | 191.2 | 10 | 121.0 | 10 | 49.0 | 48.0-50.0 |
| 17α(H),21β(H)-22R-pentakishomohopane | T35 | 482.5 | 191.2 | 10 | 121.0 | 10 | 49.5 | 48.5-50.5 |
| **Steranes** | | | | | | | | |
| 13β(H),17α(H)-20S-diacholestane | S4 | 372.7 | 217.0 | 10 | 121.0 | 10 | 34.9 | 33.9-35.9 |
| 13β(H),17α(H)-20R-diacholestane | S5 | 372.7 | 217.0 | 10 | 121.0 | 10 | 35.5 | 34.5-36.5 |
| 24-methyl-13β(H),17α(H)-20S-diacholestane (24S+R) | S8 | 386.7 | 217.0 | 10 | 121.0 | 10 | 36.4 | 35.4-37.4 |
| 24-methyl-13β(H),17α(H)-20R-diacholestane (24S+R) | S8b | 386.7 | 217.0 | 10 | 121.0 | 10 | 37.1 | 36.1-38.1 |
| 24-ethyl-13β(H),17α(H)-20S-diacholestane | S19 | 400.7 | 217.0 | 10 | 121.0 | 10 | 37.7 | 36.7-38.7 |
| 24-ethyl-13β(H),17α(H)-20R-diacholestane | S18 | 400.7 | 217.0 | 10 | 121.0 | 10 | 38.3 | 37.3-39.3 |
| 5α(H),14α(H),17α(H)-20S-cholestane | S12 | 372.7 | 217.0 | 10 | 121.0 | 10 | 37.5 | 35.5-38.5 |
| 5α(H),14α(H),17α(H)-20R-cholestane | S17 | 372.7 | 217.0 | 10 | 121.0 | 10 | 38.2 | 37.2-39.2 |
| 5α(H),14β(H),17β(H)-20S-cholestane | S15 | 372.7 | 217.0 | 10 | 121.0 | 10 | 37.9 | 36.9-38.9 |
| 5α(H),14β(H),17β(H)-20R-cholestane | S14 | 372.7 | 217.0 | 10 | 121.0 | 10 | 37.7 | 36.7-38.7 |
| 24-methyl-5α(H),14α(H),17α(H)-20S-cholestane (24S+R) | S20 | 386.7 | 217.0 | 10 | 121.0 | 10 | 39.2 | 38.2-40.2 |
| 24-methyl-5α(H),14α(H),17α(H)-20R-cholestane | S24 | 386.7 | 217.0 | 10 | 121.0 | 10 | 39.9 | 38.9-40.9 |
| 24-methyl-5α(H),14β(H),17β(H)-20R-cholestane | S22 | 386.7 | 217.0 | 10 | 121.0 | 10 | 39.3 | 38.3-40.3 |
| 24-methyl-5α(H),14β(H),17β(H)-20S-cholestane | S23 | 386.7 | 217.0 | 10 | 121.0 | 10 | 39.5 | 38.5-40.5 |
| 24-ethyl-5α(H),14α(H),17α(H)-20S-cholestane | S25 | 400.7 | 217.0 | 10 | 121.0 | 10 | 40.4 | 39.4-41.4 |
| 24-ethyl-5α(H),14α(H),17α(H)-20R-cholestane | S28 | 400.7 | 217.0 | 10 | 121.0 | 10 | 41.3 | 40.3-42.3 |
| 24-ethyl-5α(H),14β(H),17β(H)-20S-cholestane | S27 | 400.7 | 217.0 | 10 | 121.0 | 10 | 40.8 | 39.8-41.8 |
| 24-ethyl-5α(H),14β(H),17β(H)-20R-cholestane | S26 | 400.7 | 217.0 | 10 | 121.0 | 10 | 40.7 | 39.7-41.7 |
| **Triaromatic steroids (TAS)** | | | | | | | | |
| C20-triaromatic steroid | C20 | 231.0 | 203.0 | 10 | 216.0 | 10 | 30.0 | 29.5-30.5 |
| C21-triaromatic steroid | C21 | 231.0 | 203.0 | 10 | 216.0 | 10 | 31.6 | 31.1-32.1 |
| C26-20S-triaromatic steroid | C26S | 231.0 | 203.0 | 10 | 216.0 | 10 | 38.3 | 37.8-38.8 |
| C26-20R, C27-20S | C26R-C27S | 231.0 | 203.0 | 10 | 216.0 | 10 | 39.3 | 38.8-39.8 |
| C28-20S-triaromatic steroid | C28S | 231.0 | 203.0 | 10 | 216.0 | 10 | 40.2 | 39.7-40.7 |
| C27-20R-triaromatic steroid | C27R | 231.0 | 203.0 | 10 | 216.0 | 10 | 40.7 | 40.2-41.2 |
| C28-20R-triaromatic steroid | C28R | 231.0 | 203.0 | 10 | 216.0 | 10 | 42.0 | 41.5-42.5 |

Supplemental Table 2b:

Hydrocarbon compounds (PAHs, aliphatics) analyzed with analytical parameters.

| Compounds | Abbreviation | Precursor ion (m/z) | Quantitation ion (m/z) | CE 1 (eV) | Confirmation ion (m/z) | CE 2 (eV) | RT (min) | RT window width (± RT min) |
|---|---|---|---|---|---|---|---|---|
| **Polycyclic aromatics hydrocarbons (PAHs)** | | | | | | | | |
| Naphthalene | N | 128.0 | 102.0 | 20 | 127.0 | 25 | 10.7 | 10.0-11.0 |
| C1 napthalene | N1 | 142.0 | 141.0 | 20 | 115.0 | 25 | 12.8 | 11.5-14.0 |
| C2 napthalene | N2 | 156.0 | 141.0 | 20 | 115.0 | 30 | 14.8 | 13.0-16.5 |
| C3 napthalene | N3 | 170.0 | 155.0 | 20 | 127.0 | 30 | 16.5 | 13.0-20.0 |
| C4 napthalene | N4 | 184.0 | 169.0 | 20 | 154.0 | 40 | 18.4 | 16.0-21.0 |
| Acenaphythylene | ACL | 152.0 | 151.0 | 15 | 150.0 | 20 | 15.4 | 15.0-15.7 |
| Acenaphthene | ACE | 154.0 | 153.0 | 15 | 152.0 | 30 | 15.8 | 15.5-16.2 |
| Fluorene | F | 166.0 | 165.0 | 20 | 163.0 | 30 | 17.3 | 17.0-17.7 |
| C1 Fluorene | FC1 | 180.0 | 165.0 | 20 | 178.0 | 20 | 19.0 | 17.0-21.0 |
| C2 Fluorene | FC2 | 194.0 | 179.0 | 20 | 178.0 | 20 | 20.7 | 19.0-22.5 |
| Dibenzothiophene | D | 184.0 | 152.0 | 30 | 139.0 | 30 | 19.8 | 19.5-20.0 |
| C1 dibenzothiophene | D1 | 198.0 | 197.0 | 10 | 165.0 | 25 | 21.5 | 18.0-25.0 |
| C2 dibenzothiophene | D2 | 212.0 | 197.0 | 20 | 178.0 | 20 | 23.0 | 20.5-25.5 |
| Retene | Re | 234.0 | 219.0 | 10 | 204.0 | 10 | 27.0 | 26.5-27.5 |
| Anthracene | AN | 178.0 | 176.0 | 30 | 152.0 | 30 | 20.3 | 19.8-20.8 |
| Phenanthrene | P | 178.0 | 176.0 | 30 | 152.0 | 30 | 20.3 | 19.8-20.8 |
| C1 phenanthrene/anthracene | P/AN1 | 192.0 | 191.0 | 20 | 189.0 | 40 | 22.1 | 19.5-25.0 |
| C2 phenanthrene/anthracene | P/AN2 | 206.0 | 191.0 | 20 | 189.0 | 40 | 24.3 | 21.5-27.0 |
| C3 phenanthrene/anthracene | P/AN3 | 220.0 | 189.0 | 40 | 205.0 | 30 | 25.9 | 23.0-29.0 |
| C4 phenanthrene/anthracene | P/AN4 | 234.0 | 219.0 | 10 | 204.0 | 20 | 27.9 | 25.0-30.5 |
| Fluoranthene | FL | 202.0 | 200.0 | 40 | 201.0 | 30 | 24.9 | 23.4-26.4 |
| Pyrene | PY | 202.0 | 200.0 | 40 | 201.0 | 30 | 24.9 | 23.5-26.4 |
| C1 fluoranthene/pyrene | FL/PY1 | 216.0 | 215.0 | 30 | 213.0 | 40 | 27.5 | 25.0-30.0 |
| C2 fluoranthene/pyrene | FL/PY2 | 230.0 | 215.0 | 40 | 229.0 | 20 | 29.7 | 27.0-32.5 |
| C3 fluoranthene/pyrene | FL/PY3 | 244.0 | 228.0 | 40 | 229.0 | 40 | 31.7 | 29.0-34.5 |
| C4 fluoranthene/pyrene | FL/PY4 | 258.0 | 243.0 | 20 | 228.0 | 40 | 34.0 | 31.0-36.5 |
| Benz[a]anthracene | BAA | 228.0 | 226.0 | 20 | 200.0 | 40 | 31.3 | 30.9-31.7 |
| Chrysene | C | 228.0 | 226.0 | 20 | 200.0 | 40 | 31.5 | 31.1-31.9 |
| C1 benz[a]anthracene/chrysene | BAA/C1 | 242.0 | 239.0 | 40 | 241.0 | 40 | 33.7 | 29.5-38.0 |
| C2 benz[a]anthracene/chrysene | BAA/C2 | 256.0 | 239.0 | 40 | 255.0 | 20 | 35.7 | 31.5-40.0 |
| C3 benz[a]anthracene/chrysene | BAA/C3 | 270.0 | 239.0 | 50 | 255.0 | 20 | 37.9 | 33.5-42.0 |
| C4 benz[a]anthracene/chrysene | BAA/C4 | 284.0 | 239.0 | 50 | 269.0 | 50 | 39.0 | 35.0-43.0 |
| Benzo(b)fluoranthene | BBF | 252.0 | 250.0 | 40 | 251.0 | 40 | 36.8 | 36.3-37.3 |
| Benzo(k)fluoranthene | BKF | 252.0 | 250.0 | 40 | 251.0 | 40 | 37.0 | 36.6-37.5 |
| Benzo(e)pyrene | BeP | 252.0 | 250.0 | 40 | 251.0 | 40 | 38.1 | 37.6-38.6 |
| Benzo(a)pyrene | BAP | 252.0 | 250.0 | 40 | 251.0 | 40 | 38.3 | 37.8-38.8 |
| Perylene | Pe | 252.0 | 250.0 | 40 | 251.0 | 40 | 38.7 | 38.2-39.2 |
| Indeno(1,2,3)pyrene | ID | 276.0 | 274.0 | 50 | 273.0 | 50 | 43.3 | 42.8-43.8 |
| Dibenz[ah]anthracene | DA | 278.0 | 279.0 | 40 | 275.0 | 10 | 43.5 | 43.0-44.0 |
| Benzo(ghi)perylene | BGP | 276.0 | 274.0 | 50 | 273.0 | 50 | 44.3 | 43.8-44.8 |
| **Aliphatics** | | | | | | | | |
| *n* -alkanes C12-C37 | C12-C37 | 57.0 | 57.0 | 0 | ----- | 0 | 20.0 | 10.0-50.0 |
| Pristane | Pr | 57.0 | 57.0 | 0 | ----- | 0 | 18.9 | 18.8-19.0 |
| Phytane | Phy | 57.0 | 57.0 | 0 | ----- | 0 | 20.3 | 20.2-20.4 |

Supplemental Table 3: Carbon Isotope activities.

| | $^{13}C$ | | $\Delta^{14}C$ | | %C | |
|---|---|---|---|---|---|---|
| Site | 0-0.2 cm | 0-1 cm | 0-0.2 cm | 0-1 cm | 0-0.2 cm | 0-1 cm |
| 1 | -22.3 | -21.6 | -179.4 | -202.6 | 2.37 | 1.73 |
| 2 | -21.9 | -21.3 | -252.7 | -234.3 | 1.71 | 1.47 |
| 3 | -21.8 | -21.4 | -229.3 | -247.1 | 1.81 | 1.53 |
| 4 | -22.4 | -21.8 | -194.4 | -199.3 | 2.13 | 1.71 |
| 5 | -21.2 | -21.1 | -177.3 | -186.2 | 2.25 | 1.85 |
| 6 | -21.6 | -21.3 | -180.2 | -185.2 | 2.37 | 1.89 |
| 7 | -21.9 | -21.3 | -181.4 | -204.5 | 2.55 | 1.72 |
| 8 | -21.2 | -21 | -238.7 | -238.6 | 1.48 | 1.35 |
| 9 | -22.1 | -21.6 | -314.8 | -295.7 | 1.45 | 1.28 |
| 10 | -21 | -21 | -233.1 | -233.8 | 1.29 | 1.28 |
| 11 | -21.1 | -20.8 | -243.8 | -237.6 | 1.4 | 1.33 |
| 12 | -22 | -21.8 | -201.4 | -166.4 | 2.46 | 1.9 |
| 13 | -21.3 | -21 | -165 | -200 | 2.13 | 1.61 |
| 14 | -21.8 | -21.5 | -139.9 | -134.7 | 2.92 | 2.52 |
| 15 | -22.5 | -21.9 | -207.9 | -232.5 | 2.84 | 1.71 |
| 16 | -22.6 | -22.2 | -319.3 | -313.1 | 1.63 | 1.34 |
| 17 | -21.5 | -21.2 | -227.1 | -237.5 | 1.8 | 1.47 |
| 18 | -21.4 | -21 | -255.2 | -239.2 | 1.35 | 1.31 |
| 19 | -20.7 | -20.6 | -225.2 | -252.2 | 1.32 | 1.2 |
| 20 | -21.3 | -21.4 | -258.9 | -261 | 1.4 | 1.34 |
| 21 | -21.3 | -21 | -186.6 | -202.6 | 1.51 | 1.37 |
| 30 | -21.9 | -21.5 | -167 | -171 | 2.72 | 2.19 |
| DwH-01 | -21.7 | -21.5 | -211.2 | -226.3 | 1.46 | 1.41 |

Supplemental Table 4:

Benthic foraminifera density (individuals per cubic centimeter) and taphonomy (fracture percentage) by sampling station and sample depth (mm).

| Site | Depth (mm) | | | Density (indiv./cm$^3$) | Fracture Percentage |
|---|---|---|---|---|---|
| | Top | Bottom | mean | | |
| 1 | 0 | 2 | 1 | 15 | 10.6 |
| | 2 | 4 | 3 | 19 | 11.5 |
| | 4 | 6 | 5 | 19 | 9.5 |
| | 6 | 8 | 7 | 16 | 9.5 |
| | 8 | 10 | 9 | 17 | 17.2 |
| | 10 | 12 | 11 | 22 | 13.7 |
| | 20 | 22 | 21 | 24 | 11.7 |
| 9 | 0 | 2 | 1 | 22 | 12.7 |
| | 2 | 4 | 3 | 25 | 10.4 |
| | 4 | 6 | 5 | 29 | 9.8 |
| | 6 | 8 | 7 | 21 | 15.1 |
| | 8 | 10 | 9 | 30 | 15.3 |
| | 20 | 22 | 21 | 40 | 14.9 |
| 12 | 0 | 2 | 1 | 15 | 25.1 |
| | 2 | 4 | 3 | 26 | 21.0 |
| | 4 | 6 | 5 | 23 | 18.8 |
| | 6 | 8 | 7 | 21 | 21.5 |
| | 8 | 10 | 9 | 27 | 19.4 |
| | 10 | 12 | 11 | 22 | 19.7 |
| | 20 | 22 | 21 | 24 | 18.9 |
| 14 | 0 | 2 | 1 | 74 | 15.2 |
| | 2 | 4 | 3 | 18 | 17.2 |
| | 4 | 6 | 5 | 20 | 21.5 |
| | 6 | 8 | 7 | 24 | 16.7 |
| | 8 | 10 | 9 | 28 | 14.2 |
| | 10 | 12 | 11 | 61 | 12.9 |
| | 20 | 22 | 21 | 45 | 14.6 |
| 16 | 0 | 2 | 1 | 26 | 9.9 |
| | 2 | 4 | 3 | 18 | 8.4 |
| | 4 | 6 | 5 | 36 | 9.9 |
| | 6 | 8 | 7 | 33 | 12.9 |
| | 8 | 10 | 9 | 29 | 7.5 |
| | 20 | 22 | 21 | 16 | 11.5 |